

## Rapid communication

# Single-pulse time- and fluence-resolved optical measurements at femtosecond excited surfaces

K. Sokolowski-Tinten<sup>1,\*</sup>, A. Cavalleri<sup>1,2</sup>, D. von der Linde<sup>1</sup>

<sup>1</sup>Institut für Laser- und Plasmaphysik, Universität Essen, D-45117 Essen, Germany

<sup>2</sup>Dept. of Chemistry and Biochemistry, University of California, San Diego, La Jolla, CA 92093-0339, USA

Received: 16 August 1999/Accepted: 17 August 1999/Published online: 30 September 1999

**Abstract.** We describe a new technique for optical pump–probe measurements at femtosecond excited surfaces. By combining time-resolved microscopy with cylindrical focusing of the pump, complete mapping of the time and fluence dependence of laser-induced optical changes becomes possible in a single-pulse experiment.

**PACS:** 78.47.+p; 06.60.Jn

The *pump–probe* technique is a well-established method for time-resolved optical spectroscopy in the pico- and femtosecond time domain [1]. In brief, a strong *pump* pulse excites the sample, and a time-delayed *probe* pulse measures the pump-induced changes of the optical properties. Repeating the measurement at various time delays provides the complete time evolution of these changes.

However, the *traditional* pump–probe scheme suffers from several disadvantages. First, although the probe pulse is often focused to a small spot size in the central part of the excited area, spatial averaging over the probed region has to be taken into account. In particular, in situations where the optical properties of the surface are strongly inhomogeneous, averaging may lead to misinterpretation of experimental data. Second, the measurement must be repeated for each delay time and excitation fluence of interest. Therefore, a complete experimental run (over a broad time and fluence range) requires a large number of laser pulses. Third, due to statistical pulse-to-pulse variations of the laser properties (energy, pulse duration, beam profile, spatial overlap), averaging over a suitable number of laser pulses is necessary at any given delay time and fluence. The latter two points can make an experiment quite time-consuming, in particular when the repetition rate of the laser system is low. In some situations, when one is interested in nonreversible changes of materials and only small samples are available, the method cannot be applied at all.

*Time-resolved microscopy*, introduced by Downer et al. [2], partially overcomes the disadvantages of the standard pump–probe setup. The probe pulse is no longer focused onto the central part of the excited area, but serves as illumination in an optical microscope which images the area excited by the pump. This technique enables measurements with both high temporal and high spatial resolution, and therefore spatial averaging effects are avoided. In this article we describe a modification of time-resolved microscopy, which uses a cylindrical lens to focus the pump beam. We show that this technique enables complete mapping of the time *and* the fluence dependence of laser-induced optical changes in a *single-pulse* configuration.

A schematic of the experimental setup is shown in the left part of Fig. 1; the right part represents an expanded view of the excited surface area. The pump pulse strikes the sample surface at an oblique angle of incidence (in our case 45°). After adjustment of the beam diameter (we used pre-focusing with a spherical, long-focal-length lens) the pump beam is focused by a cylindrical lens, creating a line focus in the plane of incidence (POI). Therefore the intensity distribution at the surface corresponds to an elliptical Gaussian distribution with a large eccentricity (marked dark grey in the right part of Fig. 2). Within good approximation the fluence  $F$  in the central part of this distribution can be regarded as constant in the long-axis direction (parallel to the POI, here denoted as  $x$ ), but Gaussian in the direction perpendicu-

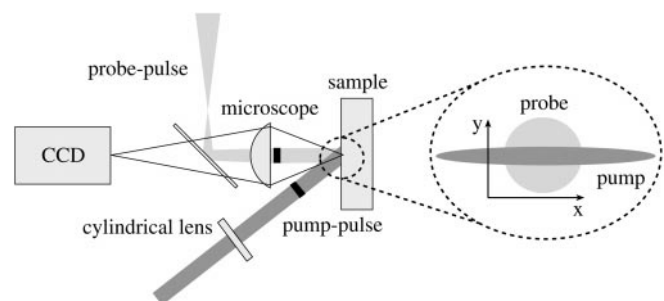


**Fig. 1.** *Left:* Schematic of experimental setup. *Right:* Expanded view of the surface. Light and dark grey mark the areas covered by the probe and the pump, respectively

\* Corresponding author.

(Fax: +49-201/183-2120, E-mail: kst@ilp.physik.uni-essen.de)

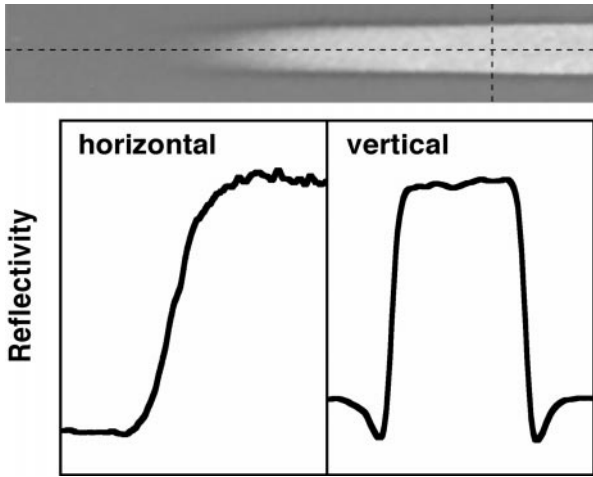


**Fig. 2.** *Top:* Picture obtained on silicon excited at approximately five times the melting threshold. *Bottom:* Horizontal and vertical cross sections (marked by the dashed lines in the picture above), which correspond to the time and the fluence dependence, respectively, of the reflectivity

lar to the POI (denoted as  $y$ ). The time-delayed probe pulse (marked with light grey) illuminates the central part of the excited surface area at normal incidence. A high-resolution microscope objective creates an image of the surface. The optical micrographs are recorded with the help of a CCD camera in conjunction with a computer-controlled video digitizer. As in a single-shot correlator for pulse-width measurements, the actual delay  $\Delta t$  between pump and probe at the sample surface varies in the  $x$  direction, because of the large difference in angle of incidence ( $45^\circ$ ), but is constant along  $y$ . Therefore, a single image of the excited surface contains information on the time *and* the fluence dependence of the reflectivity. The recorded spatial reflectivity distribution  $R(x, y)$  directly represents  $R(\Delta t, F)$ . In the experiments we used 120-fs laser pulses at 620 nm delivered by a 10-Hz-amplified colliding-pulse mode-locked (rhodamine 6G/DODCI) dye laser. The experimental geometry and the properties of the optics (numerical aperture of the microscope,  $f$  number of the cylindrical lens, etc.) have been chosen in order to achieve high temporal and spatial resolution. While the temporal resolution is given by the probe-pulse duration (120 fs), the spatial resolution (approx.  $2 \mu\text{m}$ ) determines the relative fluence resolution (approx. 3%).

To demonstrate the feasibility of this technique, ultrafast melting of femtosecond excited silicon and germanium will be discussed. This particular process has been chosen for the following reasons: (i) Melting of silicon and germanium is accompanied by a drastic increase in the reflectivity at visible and infrared wavelengths as a result of the transition from the semiconducting solid phase to the metallic liquid phase. Therefore, the phase transformation is easily detectable in an optical experiment. (ii) The optical response on silicon after intense femtosecond excitation has been carefully investigated [3, 4]. Well above threshold, melting occurs within a few hundred femtoseconds, faster than the time needed for the energy transfer between the optically excited electrons and the lattice. Since the first experiments on silicon [3], such ultrafast, *nonthermal* phase transitions have been observed in a number of covalently bonded semiconductors [4–9]. These experiments and recent theoretical work [10, 11]

have clarified the nature of the process. As first proposed by Van Vechten [12], melting is induced by an instability of the crystal lattice in the presence of the laser-excited, high-density electron–hole plasma. In summary, melting in femtosecond excited semiconductors, especially in silicon is well characterized and understood. This process will be used as an example to demonstrate the advantages of the experimental setup described above.

The upper part of Fig. 2 shows an example of an image obtained on silicon excited at approximately five times the melting threshold  $F_m = 0.17 \text{ J/cm}^2$ . As explained above, the delay time  $\Delta t$  between pump and probe increases from left to right ( $x$  coordinate) owing to the large difference in angle of incidence. The region of high reflectivity, which indicates the existence of liquid silicon, is not observed on the left side, where the probe arrives before the pump. The zone of high reflectivity is also confined in the vertical direction, corresponding to the region where the pump fluence exceeds the melting threshold  $F_m$ . Horizontal cross sections at different vertical positions provide the time dependence of the reflectivity for different pump fluences. On the other hand, vertical cross sections at different horizontal positions represent the fluence dependence of the reflectivity for different delay times between pump and probe. Examples, marked by the dashed lines in the image above, are shown in the bottom part of Fig. 2. To calibrate the time axis of the horizontal cross sections, a number of images obtained at constant fluence for different settings of the optical delay line have been compared in order to convert the space coordinate into delay time. The fluence scale (vertical space coordinate) has been calibrated by using a one-dimensional variant of a technique described by Liu [13]: For a fixed setting of the delay line the vertical extension of the molten area is plotted as a function of the square-root of the logarithm of the total pump-pulse energy. From the intersection with the energy axis, the threshold energy is obtained, and from the slope we get the vertical beam parameter.

Quantitative examples are depicted in Figs. 3 and 4. Figure 3 shows in its upper part a second image of a femtosecond-excited silicon surface. Fluence dependencies of the reflectivity are derived by using the procedure described above. They are plotted in the bottom part of Fig. 3 for three different delay times. Just after the pulse ( $\Delta t = 140 \text{ fs}$ ) the optical properties are determined by the response of the dense free-carrier plasma. At later times or at higher fluences, the increase in the reflectivity to the known value of liquid silicon is a clear indication for melting in less than 1 ps.

Figure 4 represents results obtained on germanium. In this case, time dependencies for different fluences have been extracted from horizontal cross sections of the picture shown on top. As expected, the behavior of germanium is qualitatively very similar to that of silicon. Below the melting threshold the time evolution of reflectivity is determined by the generation and relaxation of the e–h–plasma. Ultrafast melting within a few hundred femtoseconds is observed at higher fluences.

The following discussion will emphasize the *technical* aspects – advantages and limits – of our method.

- (i) According to our experience, each of the reflectivity curves shown in Figs. 3 and 4 represents the equivalent to the usual pump–probe experiment over approximately  $10^3$  laser pulses (for example, 40 delay positions,

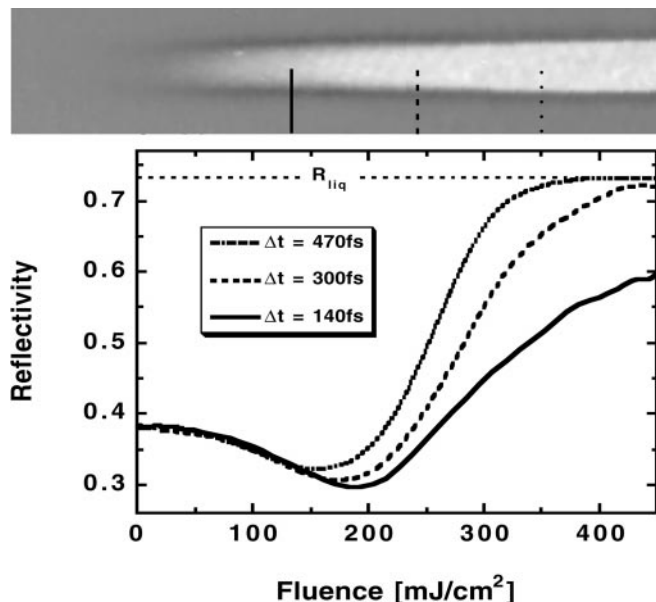


**Fig. 3.** Reflectivity of silicon as a function of the pump pulse fluence for three different delay times between pump and probe. These fluence dependencies have been obtained from vertical cross sections of the picture shown on top, as marked by the three vertical lines

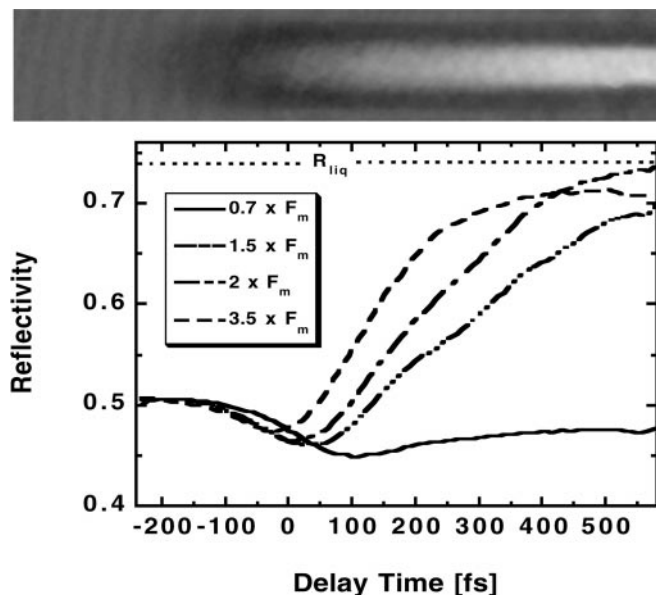


**Fig. 4.** Time evolution of the reflectivity of germanium for several pump fluences, as obtained from horizontal cross sections of the picture shown on top

25 pulses/delay). Averaging over such a large number of pulses is necessary because of pulse-to-pulse fluctuations of the laser. It has to be kept in mind that pump pulses with high intensities permanently damage the irradiated surface. Therefore the sample has to be moved between two consecutive pump pulses, and only low-repetition-rate lasers can be used (typically 10 Hz). Our single-pulse method results in an effective time-saving of three to four orders of magnitude (from 1 hour to one single pulse). In other cases, if the repetition rate is even lower or the

sample is too small to allow multi-pulse experiments, femtosecond time-resolved studies will become feasible *only* with this technique.

- (ii) The space-resolved, multi-channel detection scheme avoids spatial averaging effects.
- (iii) As a single-shot technique this method significantly reduces errors resulting from pulse-to-pulse fluctuations of the laser. For every individual pulse the recorded image represents the *complete* measurement. Moreover, changes in the beam profile and the spatial pump-probe overlap will be directly recognized, and “bad” exposures can be discarded. However, these pulse-to-pulse fluctuations currently limit the sensitivity to approximately  $\Delta R/R = 1\%$ . Better control of the laser stability together with a high-dynamic-range CCD detector (instead of the 8-bit video camera used here) will improve the accuracy.
- (iv) As mentioned above, the *time resolution* of the current setup is determined by the duration of the probe pulse (120 fs). However, to achieve a better temporal resolution it is not sufficient to decrease the pulse width. For pulses much shorter than 100 fs one has to take care of pulse distortions introduced by the aberrations of the imaging and focusing optics. The *time window* of the setup (currently 1 ps) is determined by the angle between pump and probe, and by the size of the imaged area. This *time window* can be increased by tilting the pulse front of the pump pulse by using, for example, a grating or a prism.

In summary, we have presented a modification of time-resolved microscopy, which allows time- and fluence-resolved optical measurements at femtosecond excited surfaces in a single-pulse configuration. The feasibility and the advantages and limits of the technique have been demonstrated and discussed with reflectivity measurements on silicon and germanium. The method can be readily extended to other types of (nonlinear) optical spectroscopy.

KST acknowledges support by the *Flughafen Frankfurt Main* foundation and by the University of Essen (*Forschungspool*). AC acknowledges support by the European Community (*Human Capital and Mobility*).

## References

1. for an introduction see: J.-C. Diels, W. Rudolph: *Ultrashort Laser Pulse Phenomena* (Academic Press, San Diego 1996) Chapt.9
2. M.C. Downer, R.L. Fork, C.V. Shank: *J. Opt. Soc. Am. B* **4**, 595 (1985)
3. C.V. Shank, R. Yen, C. Hirlimann: *Phys. Rev. Lett.* **50**, 454 (1983)
4. K. Sokolowski-Tinten, J. Bialkowski, D. von der Linde: *Phys. Rev. B* **51**, 14 186 (1995)
5. S.V. Govorkov, I.L. Shumay, W. Rudolph, T. Schröder: *Opt. Lett.* **16**, 1013 (1991); *Phys. Rev. B* **46**, 6864 (1992)
6. P. Saeta, J.-K. Wang, Y. Siegal, N. Bloembergen, E. Mazur: *Phys. Rev. Lett.* **67**, 1023 (1991); L. Huang, J.P. Callan, E.N. Glezer, E. Mazur: *Phys. Rev. Lett.* **80**, 185 (1998)
7. D.H. Reitze, H. Ahn, X. Wang, M.C. Downer: *Phys. Rev. B* **40**, 11 986 (1990); *Phys. Rev. B* **45**, 2677 (1992)
8. I.L. Shumay, U. Höfer: *Phys. Rev. B* **53**, 15 878 (1996)
9. H. Ahn, M.K. Grimes, X.F. Hu, M.C. Downer: In *Ultrafast Phenomena X*, ed. by P.F. Barbara, J.G. Fujimoto, W.H. Knox, W. Zinth, Springer Series in Chem. Phys. Vol. 62 (Springer, Berlin, Heidelberg 1996)
10. P. Stampfli, K.H. Bennemann: *Phys. Rev. B* **49**, 7299 (1994)
11. P.L. Silvestrelli, A. Alavi, M. Parrinello, D. Frenkel: *Phys. Rev. Lett.* **77**, 15 (1996)
12. J.A. Van Vechten, R. Tsu, F.W. Saris: *Phys. Lett. A* **74**, 422 (1979)
13. J.M. Liu: *Opt. Lett.* **7**, 196 (1982)